

A COUPLED-LINE BAND-STOP FILTER WITH THREE-SECTION TRANSMISSION-LINE STUBS AND WIDE UPPER PASS-BAND PERFORMANCE

Y. Wu* and Y. Liu

School of Electronic Engineering, Beijing University of Posts and Telecommunications, Beijing, China

Abstract—A novel band-stop filter with wide upper pass-band performance is proposed and discussed in this paper. This band-stop filter includes two three-section transmission-line stubs and a parallel coupled-line section. Because three-section transmission-line stubs and coupled-line section are used, this filter not only features good band-stop filtering property, but also has wide upper pass band. In order to verify this new filter circuit structure and its corresponding design theory, three groups of numerical examples are demonstrated. Finally, two practical band-stop filters using common microstrip technology are designed, simulated and measured. The simulated and measured results indicate that both the coupled-line section with weak coupling and two three-section stubs can improve the upper pass-band performance. Furthermore, the measured results of the second fabricated microstrip band-stop filter (Filter B) show that the 20-dB insertion-loss band-stop bandwidth at 0.46 GHz is 90 MHz and the 1.2-dB transmission coefficient upper pass band is from 0.66 GHz to 2.52 GHz. Thus, the highest pass-band frequency is extended to larger than five times of the operating center frequency of stop band.

1. INTRODUCTION

Microstrip planar-circuit filters play an important role in the design of microwave or RF sub systems. Recently, various filters with different features [1–10] have been researched widely. As significant circuit components in microwave systems, the band-stop filters are usually used to reject undesired frequency band located within the

Received 20 July 2011, Accepted 11 August 2011, Scheduled 16 August 2011

* Corresponding author: Yongle Wu (wuyongle138@gmail.com).

useful pass band. Obviously, the conventional band-stop filter [1], which is based on a quarter-wavelength open-circuit stub, has two obvious disadvantages including narrow bandwidth and an upper band-stop center frequency located at three times of the operating center frequency in the fundamental stop band. On the one hand, different bandwidth enhancement technologies for band-stop filters have been investigated in [11–18]. For examples, a cross-coupled general configuration is proposed to create a ripple and wide stop band in [11]. Signal interference techniques are also applied to design compact wideband band-stop filters in [12–14]. At the same time, modified stubs are also researched to construct wideband band-stop filters in [15, 16] while a multilayer broadside-coupled microstrip-slot-microstrip structure in [17] is used to design a band-stop filter for ultra wideband applications. In addition, multi-band band-stop filter has been developed by using transversal coupling network in [18]. On the other hand, narrow bandwidth band-stop filters are also improved by using novel microstrip technologies. For examples, a U- and V-shaped slot on the ground plane is developed to provide improved Q factors in band-stop filters [19]. Furthermore, un-modifying the ground plane, a novel defected microstrip structure by etching in-line open stubs is proposed to design microstrip narrow band-stop filter in [20]. Note that the above-mentioned band-stop filters [11–20] cannot overcome the disadvantage of the repeating stop band at odd multiples of the center frequency of fundamental stop band. In order to remove the limitation of the second harmonic response in the conventional band-stop filters, two-section stepped-impedance stubs [21, 22] and cross-coupled stepped-impedance resonators [23] are proposed in the design of band-stop filters with extended upper passbands.

Extended from the two-section stepped-impedance stubs in [21], a three-section transmission-line stub with two parallel open-circuit sub stubs and a direct-connected coupled-line section are proposed to construct a novel band-stop filter with wide upper pass band. This proposed circuit configuration has two main advantages, which are compact circuit layout and avoiding implementation of extremely-low characteristic impedance transmission lines. Because that this proposed structure including coupled-line section is symmetrical, the total external performances can be expressed by closed-form mathematical expressions. For illustrating the effects of this proposed three-section transmission-line stub, three kinds of examples for band-stop filters with single-section, two-section, and three-section stubs are designed, calculated, and compared. Their performance's comparison can emphasize the necessities of three-section stubs in the band-stop filters with wide upper pass band, as well as theoretical

verifications. Finally, an ideal bandstop filter with normal operating frequency (1 GHz) is designed, calculated, and discussed by using lossless transmission-line and coupled-line models. The ideal upper 10-dB return-loss pass-band can be extended to 5.39 GHz while the 20-dB fractional bandwidth is about 20.41% (from 0.88 GHz to 1.08 GHz). Finally, an original band-stop filter (Filter A) and the modified one (Filter B) operating at 0.5 GHz have been realized in geometry form and simulated by using full-wave planar-circuit simulation tool. For experimental verifications, Filter A and Filter B are fabricated by using common microstrip technology. The measured results of the fabricated Filter B show that the 10-dB fractional bandwidth is about 35.8% (from 0.39 GHz to 0.56 GHz) while the measured upper 8-dB return-loss pass-band bandwidth is from 0.66 GHz to 2.57 GHz.

2. THE CIRCUIT STRUCTURE AND THEORY OF THE PROPOSED BAND-STOP FILTER

According to the symmetrical network analysis results [1, 2, 6], the network analysis of Figure 1 will be simplified by analyzing the one-port networks shown in Figure 2(a) and Figure 2(b). In Figure 1 and Figure 2, Z_T is the defined real-value terminated impedance. Based on the analysis theory [1, 2, 6], the input impedances Z_{ine} and Z_{ino} shown

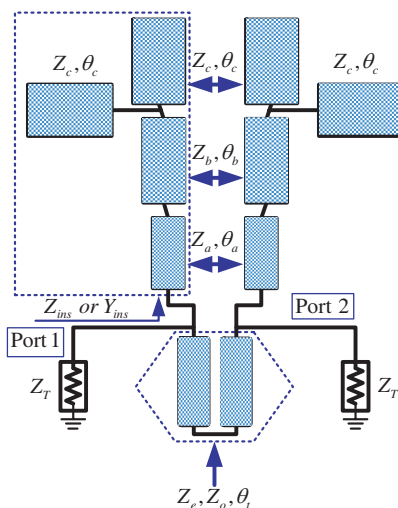


Figure 1. The proposed circuit structure of a novel band-stop filter.

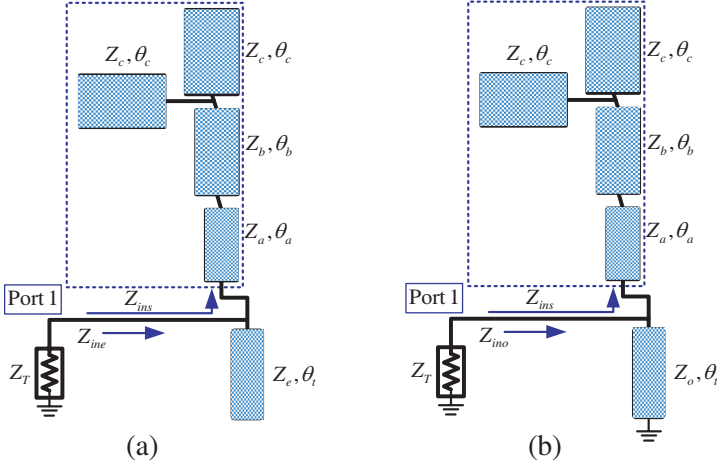


Figure 2. The equivalent simplified circuit structures of the coupled-line band-stop filter with three-section transmission-line stubs under even-mode, (a) or odd-mode, (b) excitations.

in Figure 2 can be expressed by

$$Z_{ine} = \frac{Z_{ins} \left(\frac{-jZ_e}{\tan(\theta_t)} \right)}{Z_{ins} + \left(\frac{-jZ_e}{\tan(\theta_t)} \right)}, \quad (1a)$$

$$Z_{ino} = \frac{Z_{ins}(jZ_o \tan(\theta_t))}{Z_{ins} + jZ_o \tan(\theta_t)}. \quad (1b)$$

where

$$Z_{ins1} = \frac{-jZ_c}{2 \tan(\theta_c)}, \quad (2)$$

$$Z_{ins2} = Z_b \frac{Z_{ins1} + jZ_b \tan(\theta_b)}{Z_b + jZ_{ins1} \tan(\theta_b)} = jZ_b \frac{2Z_b \tan(\theta_b) \tan(\theta_c) - Z_c}{2Z_b \tan(\theta_c) + Z_c \tan(\theta_b)}, \quad (3)$$

$$Z_{ins} = Z_{ins3} = Z_a \frac{Z_{ins2} + jZ_a \tan(\theta_a)}{Z_a + jZ_{ins2} \tan(\theta_a)}. \quad (4)$$

For convenience, the input impedance Z_{ins} can be simplified as

$$Z_{ins} = jZ_a \frac{\left(\begin{array}{l} Z_b [2Z_b \tan(\theta_b) \tan(\theta_c) - Z_c] \\ + Z_a \tan(\theta_a) [2Z_b \tan(\theta_c) + Z_c \tan(\theta_b)] \end{array} \right)}{\left(\begin{array}{l} Z_a [2Z_b \tan(\theta_c) + Z_c \tan(\theta_b)] \\ - Z_b \tan(\theta_a) [2Z_b \tan(\theta_b) \tan(\theta_c) - Z_c] \end{array} \right)}. \quad (5)$$

Therefore, the even-mode and odd-mode input impedances Z_{ine} and Z_{ino} can be expressed as

$$Z_{ine} = \frac{-j \left\{ \frac{Z_e Z_a Z_b [2Z_b \tan(\theta_b) \tan(\theta_c) - Z_c] + Z_e Z_a^2 \tan(\theta_a) [2Z_b \tan(\theta_c) + Z_c \tan(\theta_b)]}{Z_a \tan(\theta_t) [2Z_b \tan(\theta_c) + Z_c \tan(\theta_b)] - Z_b \tan(\theta_a) \tan(\theta_t) [2Z_b \tan(\theta_b) \tan(\theta_c) - Z_c]} \right\}}{\left\{ \frac{Z_a Z_b [2Z_b \tan(\theta_b) \tan(\theta_c) - Z_c] + Z_a^2 \tan(\theta_a) [2Z_b \tan(\theta_c) + Z_c \tan(\theta_b)]}{Z_a [2Z_b \tan(\theta_c) + Z_c \tan(\theta_b)]} - \frac{Z_e}{\tan(\theta_t)} \right\}}, \quad (6a)$$

$$Z_{ino} = j \frac{\left\{ \frac{Z_b Z_a Z_o \tan(\theta_t) [2Z_b \tan(\theta_b) \tan(\theta_c) - Z_c] + Z_a^2 Z_o \tan(\theta_t) \tan(\theta_a) [2Z_b \tan(\theta_c) + Z_c \tan(\theta_b)]}{Z_a [2Z_b \tan(\theta_c) + Z_c \tan(\theta_b)] - Z_b \tan(\theta_a) [2Z_b \tan(\theta_b) \tan(\theta_c) - Z_c]} \right\}}{\left\{ \frac{Z_a Z_b [2Z_b \tan(\theta_b) \tan(\theta_c) - Z_c] + Z_a^2 \tan(\theta_a) [2Z_b \tan(\theta_c) + Z_c \tan(\theta_b)]}{Z_a [2Z_b \tan(\theta_c) + Z_c \tan(\theta_b)]} + Z_o \tan(\theta_t) \right\}}. \quad (6b)$$

Then, the even-mode and odd-mode scattering parameters of this proposed band-stop filter can be calculated by [1]

$$S_{11e} = \frac{Z_{ine} - Z_T}{Z_{ine} + Z_T}, \quad (7a)$$

$$S_{11o} = \frac{Z_{ino} - Z_T}{Z_{ino} + Z_T}, \quad (7b)$$

When the above Equations (1)–(7) are applied and the symmetrical property is considered, the external scattering parameters can be expressed by [1]

$$S_{11} = S_{22} = \frac{S_{11e} + S_{11o}}{2}, \quad (8a)$$

$$S_{21} = S_{12} = \frac{S_{11e} - S_{11o}}{2}. \quad (8b)$$

By combining (7) and (8), the mathematical expressions of scattering parameters are

$$S_{11} = \frac{Z_{ine} Z_{ino} - Z_T^2}{(Z_{ine} + Z_T)(Z_{ino} + Z_T)}, \quad (9a)$$

$$S_{21} = \frac{(Z_{ine} - Z_{ino}) Z_T}{(Z_{ine} + Z_T)(Z_{ino} + Z_T)}. \quad (9b)$$

Obviously, there is a rigorous mathematical relationship that $S_{21} = 0$ at the operating frequency in ideal band-stop filters. Furthermore, the following expression can be achieved from (9b):

$$Z_{ine} - Z_{ino} = 0. \quad (10)$$

The final Equation (10) including the characteristic impedances and electrical lengths is

$$\begin{aligned} & \left\{ \frac{Z_e Z_a Z_b [2Z_b \tan(\theta_b) \tan(\theta_c) - Z_c] + Z_e Z_a^2 \tan(\theta_a) [2Z_b \tan(\theta_c) + Z_c \tan(\theta_b)]}{Z_b \tan(\theta_a) \tan(\theta_t) [2Z_b \tan(\theta_b) \tan(\theta_c) - Z_c] - Z_a \tan(\theta_t) [2Z_b \tan(\theta_c) + Z_c \tan(\theta_b)]} \right\} \\ & \times \left\{ \frac{Z_a Z_b [2Z_b \tan(\theta_b) \tan(\theta_c) - Z_c] + Z_a^2 \tan(\theta_a) [2Z_b \tan(\theta_c) + Z_c \tan(\theta_b)]}{Z_a [2Z_b \tan(\theta_c) + Z_c \tan(\theta_b)] - Z_b \tan(\theta_a) [2Z_b \tan(\theta_b) \tan(\theta_c) - Z_c]} + Z_o \tan(\theta_t) \right\} \\ & = \left\{ \frac{Z_a Z_b [2Z_b \tan(\theta_b) \tan(\theta_c) - Z_c] + Z_a^2 \tan(\theta_a) [2Z_b \tan(\theta_c) + Z_c \tan(\theta_b)]}{Z_a [2Z_b \tan(\theta_c) + Z_c \tan(\theta_b)] - Z_b \tan(\theta_a) [2Z_b \tan(\theta_b) \tan(\theta_c) - Z_c]} - \frac{Z_e}{\tan(\theta_t)} \right\} \\ & \times \left\{ \frac{Z_b Z_a Z_o \tan(\theta_t) [2Z_b \tan(\theta_b) \tan(\theta_c) - Z_c] + Z_a^2 Z_o \tan(\theta_t) \tan(\theta_a) [2Z_b \tan(\theta_c) + Z_c \tan(\theta_b)]}{Z_a [2Z_b \tan(\theta_c) + Z_c \tan(\theta_b)] - Z_b \tan(\theta_a) [2Z_b \tan(\theta_b) \tan(\theta_c) - Z_c]} \right\}. \quad (11) \end{aligned}$$

Therefore, according to the analytical Equations (1)–(9), we can calculate and analyze the external scattering parameters performance (including magnitude and phase information) of this novel band-stop filter. The band-stop performance at the operating frequency is determined by the mathematical Equation (11).

3. CHARACTERISTICS OF THE PROPOSED BAND-STOP FILTER

When the given theory of this proposed band-stop filters is considered, many numerical examples of band-stop filters with single-, two-, or three-section transmission-line stubs can be designed and calculated. Here, twelve examples are presented to show the necessities of three-section stubs in the band-stop filters with wide upper pass band. Note that all terminated impedance Z_T of the following examples is equal to 50Ω .

3.1. Band-stop Filter with Single-section Transmission-line Stubs

As the conventional band-stop filter, the three-section stubs in the proposed filter should be simplified as the single-section ones. The mathematical relationships are $Z_s = Z_a = Z_b = 0.5Z_c$ and $\theta_s = \theta_a + \theta_b + \theta_c$. The electrical parameters' values of Filters A1–A4 are given in Table 1. Based on these values, the ideal scattering parameters can be calculated by using Equations (1)–(9), and their magnitude responses are plotted in Figure 3. As shown in Figure 3, the band-stop filtering characteristic appears regularly at 1 GHz, 3 GHz, 5 GHz and so on. Therefore, the upper pass band of Filters A1–A4 are relatively narrow. In addition, it can be seen from Figure 3(a) that Filter A1 has the widest 21.8-dB return-loss pass band, which is from 1.62 to 2.38 GHz. However, the operating bandwidth at 1 GHz changes slightly for all the Filters, A1–A4, as illustrated in Figure 3(b).

Table 1. The electrical parameters' values for band-stop filters with single-section stubs ($Z_T = 50 \Omega$, $f_o = 1 \text{ GHz}$).

Figures	Example A1	Example A2	Example A3	Example A4
$Z_s(\Omega)$	50	60	50	60
Z_e	100	100	120	120
Z_o	70	70	80	80
θ_s (Degree)	90	90	90	90
θ_t	45	45	45	45

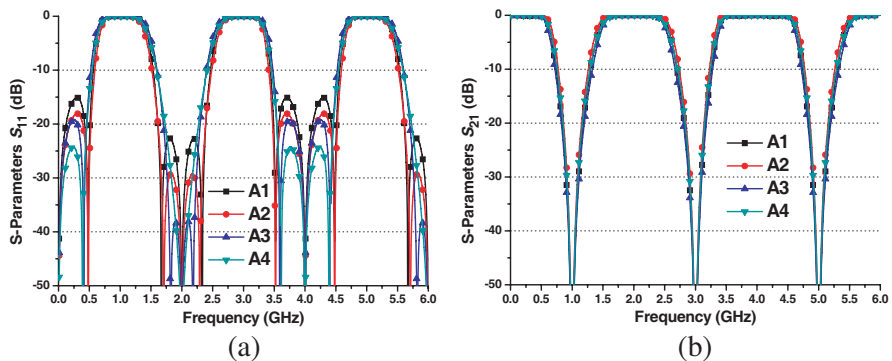


Figure 3. The scattering parameters of Filters A1–A4.

Table 2. The electrical parameters' values for band-stop filters with two-section stubs ($Z_T = 50 \Omega$, $f_o = 1 \text{ GHz}$).

Figures	Example B1	Example B2	Example B3	Example B4
$Z_s(\Omega)$	100	100	120	130
Z_c	60	50	60	30
Z_e	110	110	70	70
Z_o	75	75	44	44
θ_s (Degree)	35	35	35	29
θ_c	15	15	16	12
θ_t	45	45	45	46

3.2. Band-stop Filter with Two-section Transmission-line Stubs

According to the design approach given in [21], two-section transmission-line stubs are used to extend the upper pass band for band-stop filters. In this section, our proposed three-section transmission-line stubs can be reduced to two-section ones when $Z_s = Z_a = Z_b$ and $\theta_s = \theta_a + \theta_b$ are considered. In order to illustrate the wide upper pass-band performance, four typical examples of band-stop filters are designed. Their circuit parameters' values are listed in Table 2 while the corresponding scattering parameters are plotted in Figure 4. As listed in Table 2, Filter B4 has the lowest and highest characteristic impedances, corresponding to 30Ω and 130Ω . Meanwhile, the total electrical length of the used two-section stubs in Filter B4 is shortest in these four examples. It can be observed from Figure 4 that the upper 10-dB pass band of Filter B4 is from 2.25 GHz to 5.11 GHz. In the upper pass band of 2.25 GHz to 5.11 GHz, the transmission loss is smaller than 0.46 dB. Obviously, this proposed three-section stubs are more general cases of the previous two-section ones.

3.3. Band-stop Filter with Three-section Transmission-line Stubs

Different from the above discussed eight examples including Filters A1–A4 and B1–B4, these presented four examples such as Filters C1–C4 combine a coupled-line section and two groups of three-section transmission-line stubs. As typical examples, their electrical

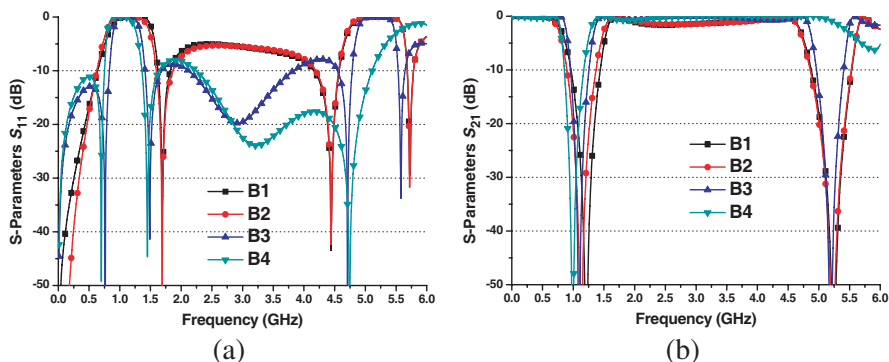


Figure 4. The scattering parameters of Filters B1–B4.

Table 3. The electrical parameters’ values for band-stop filters with three-section stubs ($Z_T = 50 \Omega$, $f_o = 1 \text{ GHz}$).

Figures	Example C1	Example C2	Example C3	Example C4
$Z_a(\Omega)$	100	120	120	138
Z_b	111	60	95	120
Z_c	40	39	33	31
Z_e	100	72	70	67
Z_o	66	41	50	58
θ_a (Degree)	33	26	16	19
θ_b	13	13	25	12
θ_c	11	12	10	11
θ_t	45	50	43	41

parameters’ values are given in Table 3 and the calculated scattering parameters are shown in Figure 5. As shown in Figure 5, Filter C1 does not perform wide upper pass band. It is very interesting that Filters C2 and C3 have different pass band. The pass band of Filter C3 is close to low-frequency band and the other one of Filter C2 is close to high-frequency band. Fortunately, after careful tuning and modifying the circuit parameters of the proposed band-stop filter, Filter C4 has the widest 10-dB return-loss upper pass band, which is from 1.44 GHz to 5.3 GHz. Note that the used characteristic impedances in Filter C4 are available for the fabrication of common microstrip technology based on common substrates.

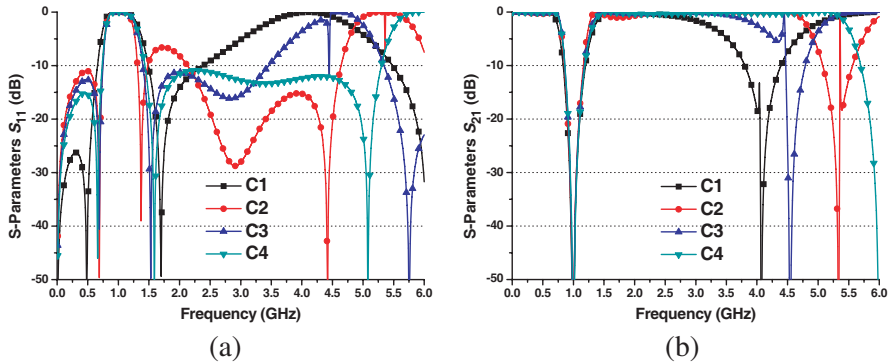


Figure 5. The scattering parameters of Filters C1–C4.

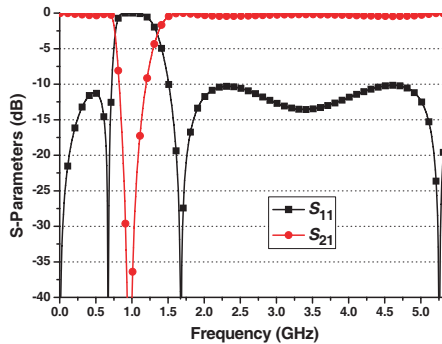


Figure 6. The ideal scattering parameter performance of the final example when the operating frequency is 1 GHz.

4. SIMULATED AND MEASURED EXAMPLES

In this section, two microstrip examples with the simulated and measured results are illustrated to verify our proposed idea. These two examples are originated from a typical one. This typical and ideal filter has the following electrical parameters: $Z_T = 50 \Omega$, $Z_a = 120 \Omega$, $Z_b = 50 \Omega$, $Z_c = 34 \Omega$, $Z_e = 74 \Omega$, $Z_o = 52 \Omega$, $\theta_a = 25^\circ$, $\theta_b = 10^\circ$, $\theta_c = 13^\circ$, $\theta_t = 40^\circ$. Based on the lossless transmission-line and coupled-line models, the calculated scattering parameters are shown in Figure 6. This ideal filter operates at 1 GHz. The 20-dB band-stop fractional bandwidth is about 20.41% (0.88 GHz–1.08 GHz). The low 10-dB return-loss pass band is from DC to 0.72 GHz while the upper 10-dB return-loss pass band is from 1.51 GHz to 5.39 GHz.

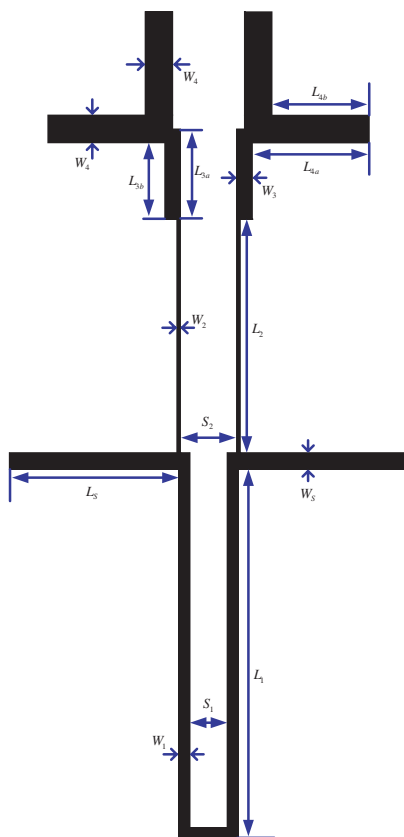


Figure 7. The physical dimension definition of the proposed microstrip band-stop filter example.

In the following microstrip examples, a practical substrate with the relative dielectric constant of 3.48 and the height of 0.762 mm is applied. Figure 7 shows the physical dimension definition of the final layout of these two fabricated band-stop filters. The operating center frequency of these two fabricated band-stop filters is 0.5 GHz. The first band-stop filter (Filter A) uses the following physical dimension values: $w_S = 1.722$ mm, $w_1 = 1.138$ mm, $w_2 = 0.226$ mm, $w_3 = 1.722$ mm, $w_4 = 3.048$ mm, $S_1 = 0.56$ mm, $S_2 = 2.84$ mm, $L_1 = 41$ mm, $L_2 = 26$ mm, $L_{3a} = 10$ mm, $L_{3b} = 8.475$ mm, $L_{4a} = 13$ mm, $L_{4b} = 10.81$ mm, $L_S = 19$ mm. The second band-stop filter (Filter B) uses the modified physical dimension values $S_1 = 4.04$ mm and $S_2 = 6.32$ mm, other dimension values are the same as those of Filter A. Figure 8 shows the practical photograph of the final fabricated microstrip Filter A and Filter B.

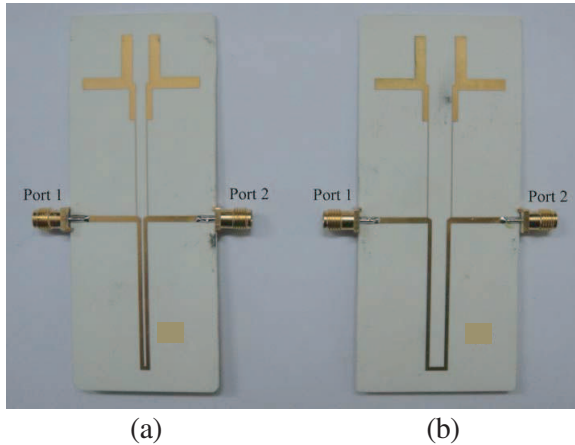


Figure 8. The photograph of the fabricated microstrip (a) Filter A, and (b) Filter B.

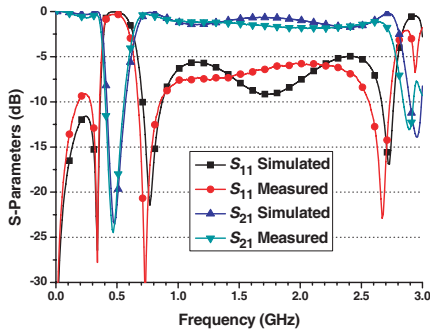


Figure 9. The simulated and measured results of Filter A (the operating frequency is 0.5 GHz).

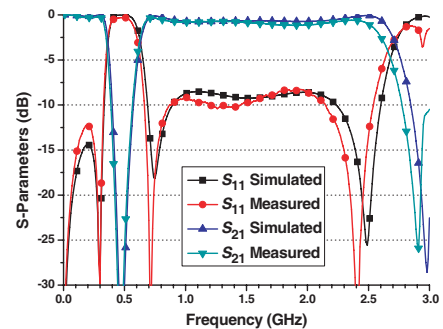


Figure 10. The simulated and measured results of Filter B (the operating frequency is 0.5 GHz).

The simulated results shown in both Figure 9 and Figure 10 are accomplished by a full-wave simulation tool while the measurement is performed by using Agilent N5230A network analyzer. As shown in both Figure 9 and Figure 10, the full-wave simulated and measured scattering parameters are in good agreement. The measured operating stop band of Filter B is centered at 0.46 GHz (ideal value is 0.5 GHz) and the highest upper 8-dB return-loss pass-band frequency is 2.57 GHz (5.58 times of the operating stop-band frequency 0.46 GHz). The measured group-delay variation in the upper pass band of 0.8 to 2.6 GHz is less than 0.75 ns, as shown in Figure 11.

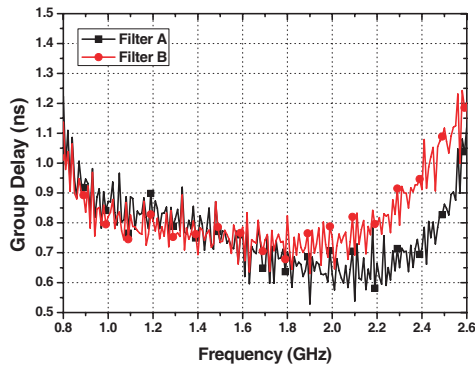


Figure 11. The measured group-delay results of Filter A and Filter B (the operating frequency is 0.5 GHz).

5. CONCLUSION

A novel circuit configuration is proposed to construct new kinds of band-stop filters with wide upper pass band. This proposed circuit configuration includes a coupled-line section and two three-section transmission-line stubs. Twelve numerical examples are designed and calculated for theoretical comparison and verifications. Furthermore, a typical and ideal band-stop filter with wide upper pass band is chosen to fabricate on the practical substrate in microstrip form. Finally, a modified band-stop filter has good simulated and measured results, indicating that our proposed idea is correct and significant. It is necessary to point out that the complete design procedure for this proposed band-stop filter is based on closed-form mathematical expressions.

ACKNOWLEDGMENT

This work was supported in part by Important National Science & Technology Specific Projects (No. 2009ZX03005-002-02 and 2010ZX03007-003-04), and the corresponding Chinese patent has been pending.

REFERENCES

1. Hong, J.-S. and M. J. Lancaster, *Microstrip Filters for RF/Microwave Applications*, Chapters 2 and 6, Wiley, New York, 2001.

2. Wu, Y., Y. Liu, S. Li, and C. Yu, "A simple microstrip bandpass filter with analytical design theory and sharp skirt selectivity," *Journal of Electromagnetic Waves and Applications*, Vol. 25, No. 8–9, 1253–1263, 2011.
3. Yu, W.-H., J.-C. Mou, X. Li, and X. Lv, "A compact filter with sharp-transition and wideband-rejection using the novel defected ground structure," *Journal of Electromagnetic Waves and Applications*, Vol. 23, No. 2–3, 329–340, 2009.
4. Wang, Y. X., "Microstrip cross-coupled tri-section stepped-impedance bandpass filter with wide stop-band performance," *Journal of Electromagnetic Waves and Applications*, Vol. 23, No. 2–3, 289–296, 2009.
5. Al-Zayed, A. S. and S. F. Mahmoud, "On the design of an improved dual operation, wide band ring resonator filter," *Journal of Electromagnetic Waves and Applications*, Vol. 23, No. 14–15, 1939–1946, 2009.
6. Wu, Y., Y. Liu, S. Li, and C. Yu, "A new wide-stopband low-pass filter with generalized coupled-line circuit and analytical theory," *Progress In Electromagnetics Research*, Vol. 116, 553–567, 2011.
7. Chen, H., Y.-H. Wu, Y.-M. Yang, and Y.-X. Zhang, "A novel and compact bandstop filter with folded microstrip/CPW hybrid structure," *Journal of Electromagnetic Waves and Applications*, Vol. 24, No. 1, 103–112, 2010.
8. Khalilpour, J. and M. Hakkak, "Controllable waveguide bandstop filter using S-shaped ring resonators," *Journal of Electromagnetic Waves and Applications*, Vol. 24, No. 5–6, 587–596, 2010.
9. Luo, X., J.-G. Ma, K. Ma, and K. S. Yeo, "Compact UWB bandpass filter with ultra narrow notched band," *IEEE Microwave and Wireless Components Letters*, Vol. 20, No. 3, 145–147, 2010.
10. Luo, X., H. Qian, J.-G. Ma, K. Ma, and K. S. Yeo, "Compact dual-band bandpass filters using novel embedded spiral resonator (ESR)," *IEEE Microwave and Wireless Components Letters*, Vol. 20, No. 8, 435–437, 2010.
11. Shaman, H. and J.-S. Hong, "Wideband bandstop filter with cross-coupling," *IEEE Trans. Microw. Theory Tech.*, Vol. 55, No. 8, 1780–1785, 2007.
12. Mandal, M. K., V. K. Velidi, S. Sanyal, and A. Bhattacharya, "Design of ultra-wideband bandstop filter with three transmission zeros," *Microwave and Optical Technology Letters*, Vol. 50, No. 11, 2955–2957, 2008.

13. Mandal, M. K. and S. Sanyal, "Compact bandstop filter using signal interference technique," *Electronics Letters*, Vol. 43, No. 2, 110–111, 2007.
14. Miguel, A. S.-S., T.-P. German, and B. Enrique, "Compact wideband bandstop filter with four transmission zeros," *IEEE Microwave and Wireless Components Letters*, Vol. 20, No. 6, 313–315, 2010.
15. Velidi, V. K., A. B. Guntupalli, and S. Sanyal, "Sharp-rejection ultra-wide bandstop filters," *IEEE Microwave and Wireless Components Letters*, Vol. 19, No. 8, 503–505, 2009.
16. Malherbe, J. A. G. and C. A. Reid, "Double resonant stub bandstop filter with pseudo-elliptic response," *Electronics Letters*, Vol. 46, No. 7, 508–509, 2010.
17. Abbosh, A. M., "Multilayer bandstop filter for ultra wideband systems," *IET Microwaves, Antennas & Propagation*, Vol. 3, No. 1, 130–136, 2009.
18. Han, S. H., X.-L. Wang, and Y. Fan, "Analysis and design of multiple-band bandstop filters," *Progress In Electromagnetics Research*, Vol. 70, 297–306, 2007.
19. Woo, D.-J., T.-K. Lee, J.-W. Lee, C.-S. Pyo, and W.-K. Choi, "Novel U-slot and V-slot DGSs for bandstop filter with improved Q Factor," *IEEE Trans. Microw. Theory Tech.*, Vol. 54, No. 6, 2840–2847, 2006.
20. Fallahzadeh, S. and M. Tayarani, "A compact microstrip bandstop filter," *Progress In Electromagnetics Research Letters*, Vol. 11, 167–172, 2009.
21. Levy, R., R. V. Snyder, and S. Sanghoon, "Bandstop filters with extended upper passbands," *IEEE Trans. Microw. Theory Tech.*, Vol. 54, No. 6, 2503–2515, 2006.
22. Alkanhal, M. A. S., "Compact bandstop filters with extended upper passbands," *Active and Passive Electronic Components*, Vol. 2008, ID 356049, 1–6, 2008.
23. Tang, W. and J.-S. Hong, "Coupled stepped-impedance-resonator bandstop filter," *IET Microwaves, Antennas & Propagation*, Vol. 4, No. 9, 1283–1289, 2010.